Research article

X-RAY SPECTROMETRY

Received: 4 March 2014 Revised: 24 April 2014 Accepted: 28 April 2014 Published online in Wiley Online Library: 9 June 2014

(wileyonlinelibrary.com) DOI 10.1002/xrs.2544

Optimized energy dispersive X-ray fluorescence analysis of atmospheric aerosols collected at pristine and perturbed Amazon Basin sites

Andréa Arana,[a]* Ana L. Loureiro,[b] Henrique M. J. Barbosa,[b] Rene Van Grieken[c] and Paulo Artaxo[b]

Elemental composition of aerosols is important to source apportionment studies and to understand atmospheric processes that influence aerosol composition. Energy dispersive X-ray fluorescence spectroscopy was applied for measuring the elemental composition of Amazonian atmospheric aerosols. The instrument used was a spectrometer Epsilon 5, PANalytical B.V., with tridimensional geometry that reduces the background signal with a polarized X-ray detection. The measurement conditions were optimized for low-Z elements, e.g. Mg, Al, Si, that are present at very low concentrations in the Amazon. From Na to K, our detection limits are about 50% to 75% lower than previously published results for similar instrument. Calibration was performed using Micromatter standards, except for P whose standard was produced by nebulization of an aqueous solution of KH_2PO_4 at our laboratory. The multi-element reference material National Institute of Standards and Technology–2783 (air particulate filter) was used for evaluating the accuracy of the calibration procedure of the 22 elements in our standard analysis routine, and the uncertainty associated with calibration procedures was evaluated. The overall performance of the instrument and validation of our measurements were assessed by comparison with results obtained from parallel analysis using particle-induced X-ray emission and another Epsilon 5 spectrometer. The elemental composition in 660 samples collected at a pristine site in the Amazon Basin and of 1416 samples collected at a site perturbed by land use change was determined. Our measurements show trace elements associated with biogenic aerosols, soil dust, biomass burning, and sea-salt, even for the very low concentrations as observed in Amazonia.

Introduction

Quantification of atmospheric aerosol sources and processes is important because of their direct and indirect effects on climate.[1] The climatic effects of aerosols in Amazonia have been the focus of recent research.[2,3] Under natural conditions, biogenic particles dominate the picture,[4,5] with soil dust and sea-salt being minor components in the wet season.[6,7] Recent studies at remote sites of Amazonia, as Balbina[8] and Rebio Cuieiras-ZF2,[9] found PM_{10} concentrations of about 10 to 15 $\mu g\,m^{-3}$ during the wet season (January to March) in agreement with previous findings that these regions represent pristine atmospheric conditions.[10] During the dry season (August to October), however, biomass burning emissions dominate particle population, especially in areas such as Rondônia and Pará states,[11] emitting large amounts of fine mode aerosols[2] disrupting the natural conditions. This large variation in aerosol concentrations represents a challenge for the sampling procedure and to the analysis methodology.

Various analytical methods for trace element analysis have been applied in environmental studies, such as, inductively coupled plasma mass spectrometry (ICP mass spectrometry), ICP optical emission spectrometry (ICP optical emission spectrometry), particle induced X-ray emission (PIXE), and wavelength-dispersive X-ray fluorescence analysis, to name a few. These techniques have advantages and disadvantages. ICP techniques have excellent detection limits (DLs) but involve sample preparation that in general leads to the destruction of the aerosol samples. PIXE requires a nuclear particle accelerator, a very large and expensive instrument.[12,13] Wavelength-dispersive X-ray fluorescence analysis has a moderate cost, but in general, the high current used in the X-ray tube can lead to losses of volatile compounds or sample destruction. A good alternative is the energy dispersive X-ray fluorescence (EDXRF),[14–16] a relatively low cost nondestructive technique that does not require further sample treatment and used in a wide range of applications (aerosols, vegetal species, electronic components, etc.).[17] Another advantage of EDXRF is the simultaneous measurement of the whole spectrum and the use of the peak area to determine the concentration of an element. The setups involve three-dimensional geometry in combination with a polarized X-ray beam to reduce the background signal.[18,19] This is important because trace element concentrations in Amazonia wet seasons are very low.[2] The Epsilon 5, a commercially available EDXRF machine from PANanalytical, has been used for quantitative analysis of atmospheric aerosols with samples collected in Belgium.[20] A more recent study which compared PIXE and

* *Correspondence to: Andréa Arana, Instituto Nacional de Pesquisas da Amazônia, Manaus, Brazil. E-mail: andreaarana@inpa.gov.br*

a *Instituto Nacional de Pesquisas da Amazônia, Manaus, Brazil*

b *Instituto de Física, Universidade de São Paulo, Rua do Matão, Travessa R, 187, CEP 05508-090, São Paulo, São Paulo, Brazil*

c *Department of Chemistry, University of Antwerp, Universiteitsplein 1, B-2610, Antwerp, Belgium*

EDXRF results for particulate matter collected in Italy showed good agreement for Al, Si, S, K, Ca, Fe, Cu, and Zn.[21]

This paper focuses on the use of EDXRF for quantitative determination of elemental concentration in atmospheric aerosols collected in a pristine and a perturbed site in Amazonia during the dry and wet seasons. This study was performed with an Epsilon 5, PANalytical B.V. instrument from the Laboratory of Atmospheric Physics at the University of São Paulo (USP). Special care was paid to optimizing DLs and accuracy for a large range of trace elements determination, accomplished by tuning sampling time, secondary target option, spectral lines used, and the current and voltage in the X-ray tube anode. The results were compared with those of PIXE and another EDXRF instruments.

Materials and methods

Aerosol samples were collected on 47 mm polycarbonate filters using a Norwegian Institute for Air Research stacked-filter unit [14] during the dry (August to October) and wet (January to March) seasons in Amazonia. The combination of filters with 0.4 and 8 μm pore sizes allowed the separation between the fine ($PM_{2.5}$) and coarse (PM_{10}) modes with a flow rate of 17 l min^{-1}. The effective collection area is 14.4 cm^2. The pristine monitoring station was set up on the large-scale biosphere atmosphere experiment site at the Reserva Biológica de Cuieiras (2°35′22″ S, 60°06′55″ W) at about 80 km north of Manaus/AM. The site, operated by Instituto Nacional de Pesquisas da Amazônia (INPA), has a total area of 22 735 ha of primary rain forest[22] with canopy heights of 35 to 40 m in the plateau region. From February 2008 to December 2011, 660 aerosol samples were collected without interruptions. Sampling time varied from 110 ± 56 h during the dry season to 120 ± 61 h during the wet season. The perturbed site is located in the state of Rondônia, where significant land use changes took place at about 10 km from downtown Porto Velho (8°41′11.92″ S, 63°51′59.73″ W). The station was operated continuously between September 2009 and October 2012, with 1416 aerosol samples collected without interruptions. Sampling time varied from 44 ± 30 h during the dry season to 100 ± 30 h during the wet season.

The EDXRF was applied for the determination of the aerosol elemental composition of each sample using an Epsilon 5, PANalytical B.V. instrument. The X-ray tube anode operates with accelerating voltages of 25–100 kV and currents of 0.5–24 mA, with a maximum power of 600 W. The primary target is Sc/W, and 11 secondary targets (Mg, Al, Si, Ti, Fe, Ge, Zr, Mo, Ag, CaF_2, and CeO_2) can be chosen for measuring different range of elements. The tridimensional polarized-beam geometry reduces the incidence of spurious scattered radiation from the X-ray tube into the detector, thus reducing the background and allowing the measurement of light and heavy elements at very low concentrations (1–30 ng cm^{-2}). A Si(Li) detector with a resolution of 126 eV for Mn K_α was used. Further details are given by Brouwer.[18,19,23]

It is important to choose a good combination of secondary target, voltage, current, and measurement time in order to optimize DLs for each element. The choice of secondary target was made in our laboratory by analysing the DL and the ability to discriminate the K_α line of interest. The measurement time was found as a commitment between a reasonable total measurement time and the DLs for each element. For instance, the elements from Na to K were measured with 600 s integration time, whereas 300 s was used for elements Ca to Pb. Table 1 shows the analysis parameters for all elements. The accelerating voltage and current were fixed for each secondary target to reduce the number of different irradiation conditions. This is important as the system allows measuring several elements under the same irradiation conditions. The total measurement time of our tuned routine analysis is only 1 h per filter. Additionally, a careful study of overlapping X-ray lines was carried out, aiming at minimizing the interference between elements. For instance, as the lines As K_α (10.53 KeV) and Pb L_α (10.55 KeV) are too close to be resolved within the instrument resolution, the line Pb $L_{\beta1}$ (12.62 KeV) was used instead in Pb concentration calculations. The area of a peak profile, integrated over the width at half maximum, gives the intensity which is used to calculate the concentration of an element. This is performed automatically by the Epsilon 5 Software, version 2.0M/ICSW 2.10, using an algorithm based on analysis of X-ray spectrum by iterative least-square fitting.[23]

The DL, the lowest measurable mass for each element according to the specific measurement conditions (secondary target, current, voltage, and background), is an important performance parameter to characterize XRF instruments.[24] After the best measurement conditions for each element were determined and the instrument was calibrated, the DL was calculated as three times the square-root of the background noise from the measurement of ten blank filters.[20] In terms of the quantities measured at the Epsilon 5, PANalytical B.V, instrument, this is

Table 1. Measurement conditions used in the EDXRF Epsilon 5, PANalytical B.V. instrument for the 23 elements determined in the protocol for routine aerosol measurements

	Secondary Target	Line	Accelerating voltage (kV)	Current (mA)
Na	Al	K_α	25	24
Mg	Si	K_α	25	24
Al	CaF_2	K_α	25	24
Si	CaF_2	K_α	25	24
P	CaF_2	K_α	25	24
S	CaF_2	K_α	25	24
Cl	CaF_2	K_α	25	24
K	CaF_2	K_α	25	24
Ca	Fe	K_α	40	15
Ti	Fe	K_α	40	15
V	Fe	K_α	40	15
Cr	Fe	K_α	40	15
Mn	Ge	K_α	75	8
Fe	Ge	K_α	75	8
Ni	Ge	K_α	75	8
Cu	Ge	K_α	75	8
Zn	Ge	K_α	75	8
As	Zr	K_α	100	6
Se	Zr	K_α	100	6
Br	Zr	K_α	100	6
Rb	Zr	K_α	100	6
Sr	$Al2O_3$	K_α	100	6
Zr	$Al2O_3$	K_α	100	6
Mo	$Al2O_3$	K_α	100	6
Cd	$Al2O_3$	K_α	100	6
Sb	CeO_2	K_α	100	6
Pb	Zr	Lb1	100	6

$$DL = \frac{3}{s_i}\sqrt{\frac{r_b}{t_b}} \quad (1)$$

where s_i is the sensitivity (counts per second divided by concentration, for the standards), r_b is the background counts per second, and t_b is the measurement time. Therefore, the DL is given in units of concentration (ng cm^{-2}).

The instrument calibration was performed with both single and multi-element standards from Micromatter Inc. (Vancouver, BC, Canada), with concentrations ranging from 5.2 to 59 μg cm^{-2}, with 5% uncertainty in the gravimetrically determined masses. These thin film standards, deposited on Nuclepore substrates and commercially available for almost all the elements from Na to Pb, are recommend by the US Environmental Protection Agency as they closely resemble the particulate layer on a filter.[25] However, these and most commercially available XRF standards have concentrations significantly larger than that found in aerosol samples from Amazonia. For element P, which plays a fundamental role in the nutrient cycle, extra care in obtaining its calibration curve was taken. Four extra standards were produced in our laboratory through the nebulization of an aqueous solution of KH_2PO_4, with mass concentrations of 3.41 ± 0.55, 7.3 ± 1.2, 8.2 ± 1.3, and 11.8 ± 1.9 μg cm^{-2}. The technique used is similar to other studies, e.g. Vanhoof *et al.*[26] The multi-element standard NIST-2783 (air particulate filter) was used to evaluate the accuracy of the calibration procedure.

As part of the quality assurance procedures, subsets of samples from this study were also analysed by PIXE and a second Epsilon 5, PANalytical B.V. instrument from Companhia Ambiental do Estado de São Paulo (CETESB), aiming to compare DLs and concentrations. For this procedure, a subset of 140 samples from Porto Velho was also measured through PIXE. The PIXE analysis was performed in a dedicated 5SDH Pelletron accelerator facility, at the Laboratório de Análise de Materiais por Feixes Iônicos in the USP, with a proton beam of 2.6 MeV. Two X-ray detectors are used in this system, one optimized for light and the second for heavy elements, providing better DLs and avoiding some of the pile-up and dead time corrections. PIXE spectra were fitted with the analysis of X-ray spectrum by iterative least-square fitting software package.[27] Further details can be found in Artaxo and Orsini.[12] Gerab *et al.*[28] discussed the validation of PIXE results from this system using other techniques such as particle-induced gamma emission and ion chromatography.

Results and discussion

The system was calibrated according to the discussed protocol. The calibration curves for Na, Al, P, Ti, Fe, and Pb elements usually present in aerosol samples are shown in Fig. 1 with the corresponding linear fitting. The regressions are all statistically significant at a confidence level of 95%, and the adjusted R-square coefficients found are all between 0.9351 and 0.9989, which correspond to a low root mean square error of about 0.17 to 2.3 μg cm^{-2}. The calibration coefficients for all determined elements are shown in Table 2. The relative error from the calibration fitting is less than 4% for all elements. This error is within the sampling errors for aerosols and is adequate for the elemental analysis.[29] The NIST-2783 reference aerosol sample was measured ten times in order to verify the accuracy of the calibration (Table 3). The variability of trace element determination was also checked with this procedure. Statistical analysis using Welch's *t*-test shows that for the elements Mg, Al, Si, K, Ca, Ti, V, Cr, Mn, Fe, Ni, Cu, Zn As, Rb, Sb, and Pb, the measured concentrations are within NIST certified values. For the elements Na, S, and Zn, there was a statistical disagreement between certified and measured concentrations, and a cause for this could not be identified.

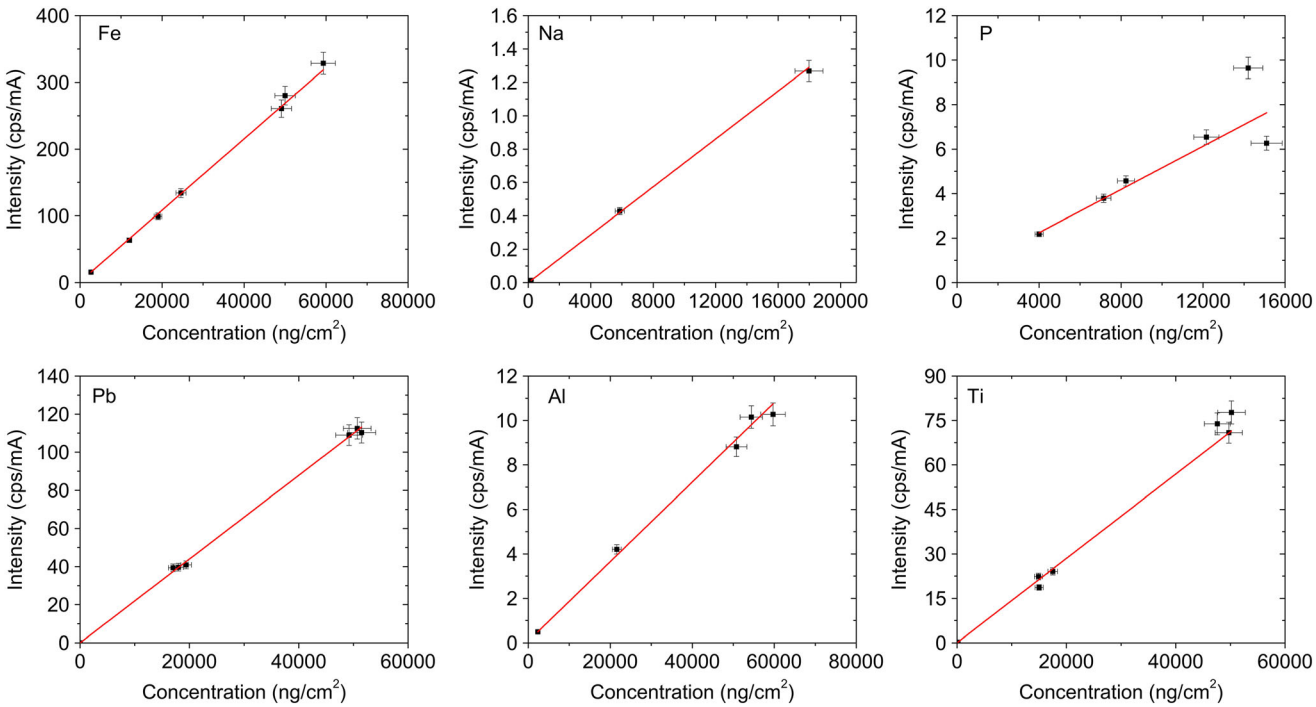

Figure 1. Calibration curves for Fe, Na, P, Pb, Al, and Ti with fitting results, which consider a 5% uncertainty in the reported concentration from single element MicroMatter standards. As discussed in the text, P standards were produced in our laboratory and have an uncertainty better than 2%. The two outliers are old multi-elemental standards from MicroMatter.

Table 2. Calibration coefficients (cps mA ng^{-1} cm^2) for each element, with the absolute and relative uncertainties

	Calibration coefficients (cps mA ng^{-1} cm^2)	%
Na	7.18E-05 ± 2.59E-06	3.61
Mg	1.39E-04 ± 3.66E-06	2.63
Al	1.79E-04 ± 4.84E-06	2.70
Si	3.48E-04 ± 1.32E-05	3.79
P	4.86E-04 ± 2.29E-05	4.71
S	1.60E-03 ± 4.04E-05	2.53
Cl	2.54E-03 ± 1.02E-04	4.02
K	4.70E-03 ± 8.38E-05	1.78
Ca	1.99E-03 ± 5.47E-05	2.75
Ti	1.42E-03 ± 2.93E-05	2.06
V	1.80E-03 ± 4.50E-05	2.50
Cr	2.50E-03 ± 6.27E-05	2.51
Mn	4.34E-03 ± 1.25E-04	2.88
Fe	5.35E-03 ± 1.27E-04	2.37
Ni	8.23E-03 ± 2.06E-04	2.50
Cu	9.22E-03 ± 1.89E-04	2.05
Zn	1.16E-02 ± 3.02E-04	2.60
Br	7.93E-03 ± 2.81E-04	3.54
Rb	1.04E-02 ± 1.48E-05	0.14
Pb	2.20E-03 ± 4.49E-05	2.04

Table 3. Comparison of the NIST 2783 reference value and the mean value measured with the EDXRF Epsilon 5, PANalytical B.V.

	Reference	Measured	*t*-test
Na	186 ± 9	131 ± 12	3.67
Mg	865 ± 43	835 ± 43	0.49
Al	2330 ± 116	2600 ± 40	2.21
Si	5883 ± 294	5780 ± 90	0.33
P	—	87 ± 2	—
S	105 ± 5	133 ± 3	4.80
Cl	—	24.5 ± 0.3	—
K	530 ± 26	570 ± 8	1.47
Ca	1325 ± 66	1380 ± 15	0.79
Ti	150 ± 7.5	168 ± 1	2.38
V	4.9 ± 0.2	1.6 ± 1.2	2.71
Cr	13.6 ± 0.7	14.5 ± 0.4	1.12
Mn	32.1 ± 1.6	33 ± 2	0.35
Fe	2661 ± 133	2900 ± 30	1.72
Ni	6.8 ± 0.3	6.3 ± 0.6	0.75
Cu	40 ± 2	43.3 ± 0.5	1.60
Zn	179 ± 9	220 ± 2	4.45
As	1.2 ± 1	1.9 ± 2.1	0.30
Se	—	5.3 ± 1.3	—
Rb	2.4 ± 0.1	0.2 ± 0.9	2.43
Sr	—	0.4 ± 4.1	—
Sb	7.2 ± 0.4	0 ± 8.6	0.84
Pb	31 ± 2	27 ± 6	0.63

Uncertainties given are the standard deviation of different measurements. Values are in ng cm^{-2}. Compatible values are those for which the Welch's *t*-test score is less than 3.

The DL for each element was calculated with (Eqn (1)) from the measurements of ten blank filters. Results for each element are shown in Table 4. Highest values are around 45 ng cm^{-2}, with most below 10 ng cm^{-2}. Assuming 24 h collection time, the atmospheric concentration corresponding to the DL was calculated and is shown in the fifth column. This result shows that indeed, the EDXRF technique is suitable for measuring aerosol samples from Amazonia, where very low concentrations are found for most months of the year. For testing the background noise distribution, the blank filters were also measured with twice the integration time for all elements. The DL was reduced by 25 ± 6% in agreement with the expected $1/\sqrt{2}$. For comparison, results from Spolnik *et al.*,[18] who used the same technique but with a different X-ray tube (Gd tube), measurement conditions (e.g. Ge-detector), and calibration standards, hence in a system that was rather optimized for heavy elements, are also shown in Table 4. Our DLs are lower for all elements except Sr, Cd, and Pb, and we are able to measure Na, Mg, P, Br, and Rb. This was achieved by tuning and calibrating the instrument for the typical low concentrations found in Amazonia as described in the previous section.

Table 4. The detection limits for the EDXRF Epsilon 5, PANalytical B.V. instrument calculated with (Eqn (1)) using the background count rate and those determined by Spolnik *et al.*[20]

	Detection limits (ng cm^{-2})			24 h Detection limits (ng m^{-3})	
	Blank	Spolnik *et al.*[20]	Fitting procedure (see text)	Blank	Fitting procedure (see text)
Na	28	—	48	17	28
Mg	30	—	49	18	29
Al	9	32	11	5.3	6.5
Si	7	30	11	4.1	6.5
P	2	—	5.1	1.4	3.0
S	2	8	5.7	1.3	3.4
Cl	2	6	3.4	1.0	2.0
K	1	5	2.7	0.86	1.6
Ca	2	4	5.6	1.1	3.3
Ti	3	3	3.5	5.4	2.1
V	3	2	2.2	1.8	1.3
Cr	2	5	1.9	0.92	1.1
Mn	3	4	2.6	1.8	1.5
Fe	2	8	3.6	1.1	2.1
Ni	1	3	1.9	0.66	1.1
Cu	2	3	2.6	0.94	1.5
Zn	1	4	2.3	0.75	1.4
As	4	3	—	2.6	—
Se	4	9	6.4	2.6	3.8
Br	3	—	5.5	1.8	3.2
Rb	6	—	—	1.8	—
Sr	16	3	25	9.6	15
Cd	20	10	—	12	—
Sb	10	20	—	6.2	—
Pb	6	8	5.5	3.6	3.2

The fourth column shows the detection limits from the fits as discussed in the text. The values shown in ng m^{-3} were calculated for 24 h sampling time.

The DL can also be estimated from the analysis of the measured samples. A subset of 136 samples from Porto Velho and 51 from Manaus was irradiated three times, and the scatter plots of the standard deviations by the average concentration for some elements are shown in Fig. 2. As the concentration decreases and

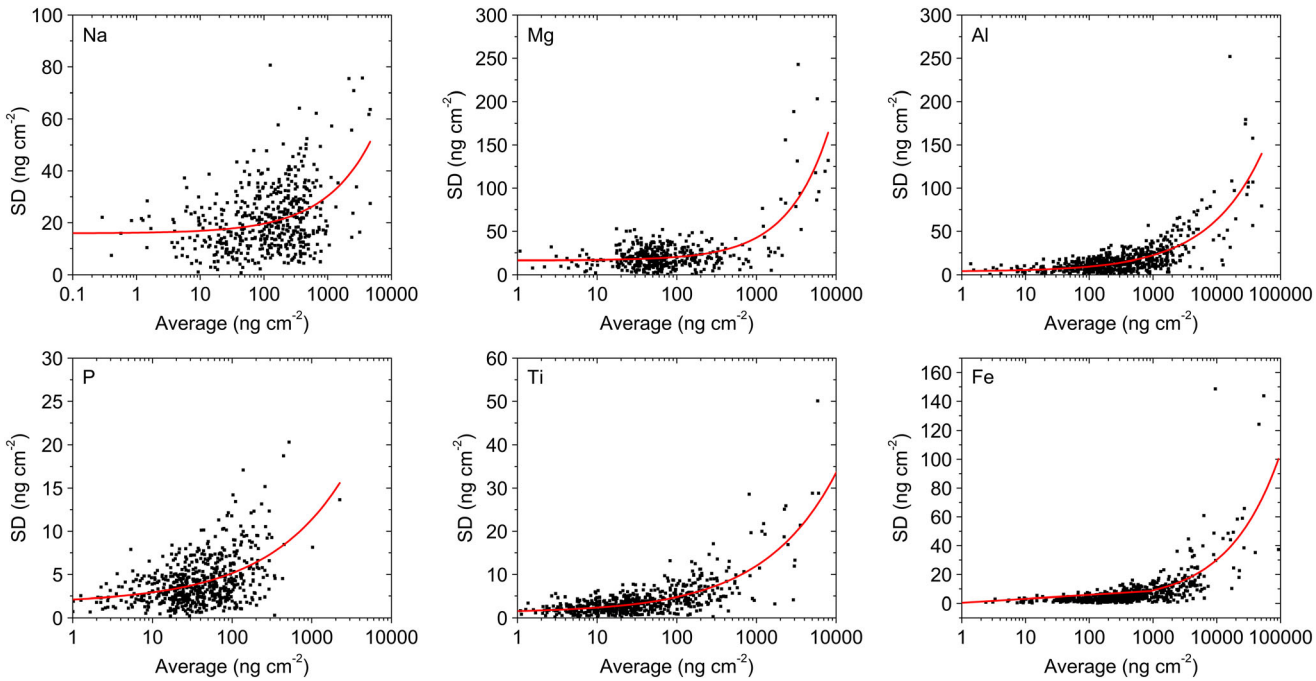

Figure 2. Standard deviations (ng cm^{-2}) as a function of the mean concentration (ng cm^{-2}) from 628 samples that were measured three times each are shown for Na, Mg, Al, P, Ti, and Fe. The adjusted R^2 and fitted parameters for the empiric function used, $Y = a + b\ (\log x)^c$, are shown in each panel.

approaches the DL, the standard deviation stabilizes as expected. The DL is calculated as three times this limit value for the uncertainty, obtained from the empirical nonlinear fit, $y = a + b\ (\log x)^c$, shown in Fig. 2. The estimated values are given in the last column of Table 4. There is a good agreement with the values from the background noise on blank filter measurements, except for P, Cl, V, Cr, and Pb. For these elements, the small range of concentrations close to the DL did not allow a reliable nonlinear fit analysis as shown by the large uncertainty in the estimated DL.

For validating our EDXRF measurements, some samples collected in Rondônia, with a relatively heavy loading, were also analysed independently using PIXE. Each sample consisted of a fine or a coarse mode Nuclepore filter, with mass concentration varying from 0.8 to 35 μg m^{-3}. Results of this comparison for some elements are shown in Fig. 3. The comparison provided a good agreement for most of the elements. Fe, for instance, provided a slope of 1.06 and R^2 of 0.96. Even an element that appears in low concentration, such as P, had a slope of 1.04, and R^2 of 0.97, a surprising result because the P Kα line is in between Si and S, elements that appear in high concentrations and that makes the fitting difficult. In the case of P and Cl, for which the NIST-2783 could not be used as a reference because of lack of certification, the agreement between PIXE and EDXRF indicates the proper standard preparation and calibration

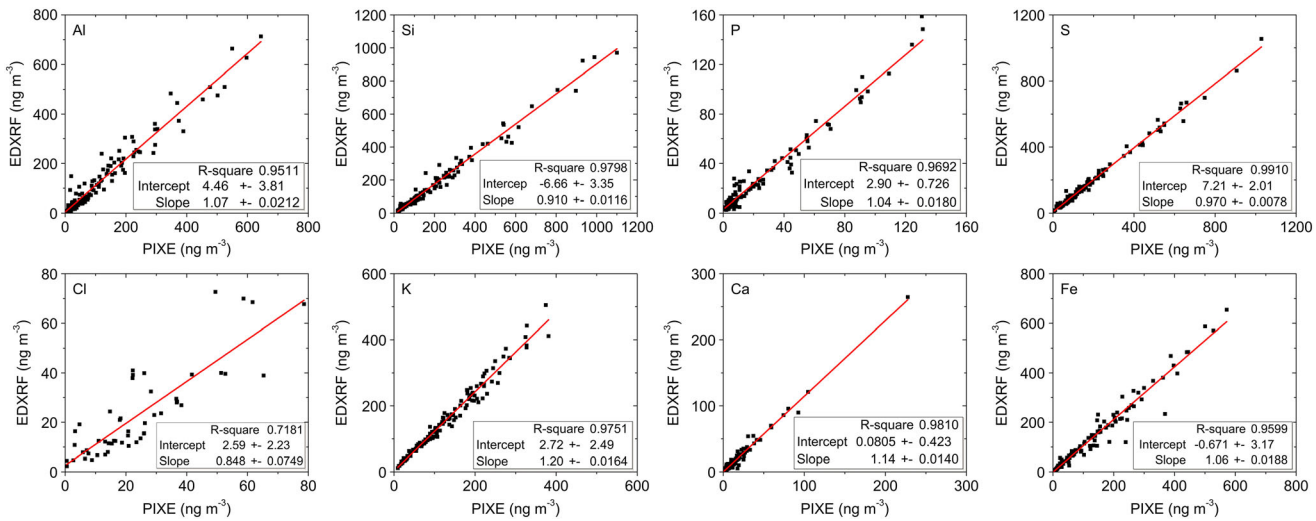

Figure 3. Comparison of PIXE and EDXRF results from 140 samples for Al, Si, P, S, Cl, K, Ca, and Fe. The intercept, slope, and adjusted R^2 are reported in each panel.

procedure developed for P calibration. For trace elements such as Cr, Mn, Cu, Br, and Pb, the correlation coefficient varied from 0.72 to 0.99. For these elements that appear close to the DL and have significant blank values, the comparison PIXE *versus* EDXRF was satisfactory, taking into account all the difficulties in quantifying elements close to the DL.[21]

A careful comparison of elemental concentrations was also performed with a similar EDXRF instrument from the University of Antwerp (UA), Belgium. This second EDXRF (called UA-Antwerp) has been used for more than 10 years,[20] rather for heavy element determinations, and was configured and calibrated with completely independent procedures. Particularly, it uses different secondary targets, a 300 s integration time for all elements and the determination of Pb and Sb is performed with different X-ray lines. Twenty-four samples from Manaus/AM (clean and pristine), Porto Velho/RO (biomass burning loaded samples), and São Paulo/SP (industrial and vehicular emissions) were measured independently with both instruments. Samples included fine and coarse mode filters, with concentrations varying from 0.7 to 70 $\mu g\,m^{-3}$. Another independent comparison was carried out with a similar Epsilon 5, PANalytical B.V. instrument from the environmental monitoring agency for the state of São Paulo (CETESB). This CETESB EDXRF instrument is used for routine air quality analysis and has a configuration similar to the one in this study but was calibrated independently. Table 5 shows the comparison of the analyses carried out with samples analysed in our instrument with these two other independent instruments.

Table 5. Comparison of elemental concentrations measured by the EDXRF Epsilon 5, PANalytical B.V. instrument at our laboratory with those measured at the University of Antwerp and at CETESB

	UA × LFA	CETESB × LFA
Al	0.80 ± 0.01	0.94 ± 0.01
Si	1.03 ± 0.01	1.00 ± 0.01
P	—	1.28 ± 0.07
S	0.73 ± 0.01	1.06 ± 0.01
Cl	0.61 ± 0.06	1.16 ± 0.04
K	1.14 ± 0.05	1.01 ± 0.01
Ca	1.17 ± 0.01	1.00 ± 0.01
Ti	1.07 ± 0.02	0.96 ± 0.04
Fe	0.84 ± 0.01	1.00 ± 0.01
Cu	1.10 ± 0.07	1.44 ± 0.10
Zn	1.08 ± 0.02	1.01 ± 0.05

Values shown are the angular coefficient and uncertainty from a linear fitting based on 24 aerosol samples collected in São Paulo, Porto Velho, and Manaus.
UA, University of Antwerp; LFA, Laboratory of Atmospheric Physics; CETESB, Companhia Ambiental do Estado de São Paulo.

With the CETESB EDXRF, the angular coefficients shown in Table 5 are within 0.94 and 1.16, except for P and Cu that had concentrations close to the DL. This good comparison was expected as both instruments were similarly optimized for measuring light elements with low concentrations. With the UA system, values ranged from 0.61 to 1.17 with angular coefficients closer to 1 for heavier elements and close to 0.7 for lighter elements. The reason for these differences could be explained by the fact that the UA instrument was optimized for heavy elements. The agreement between the instruments is very good overall, taking into account the differences in procedures and differences in the configuration of the XRF instruments.

Our EDXRF system is mostly used for trace element determination for aerosol particles in Amazonia. After the calibration and

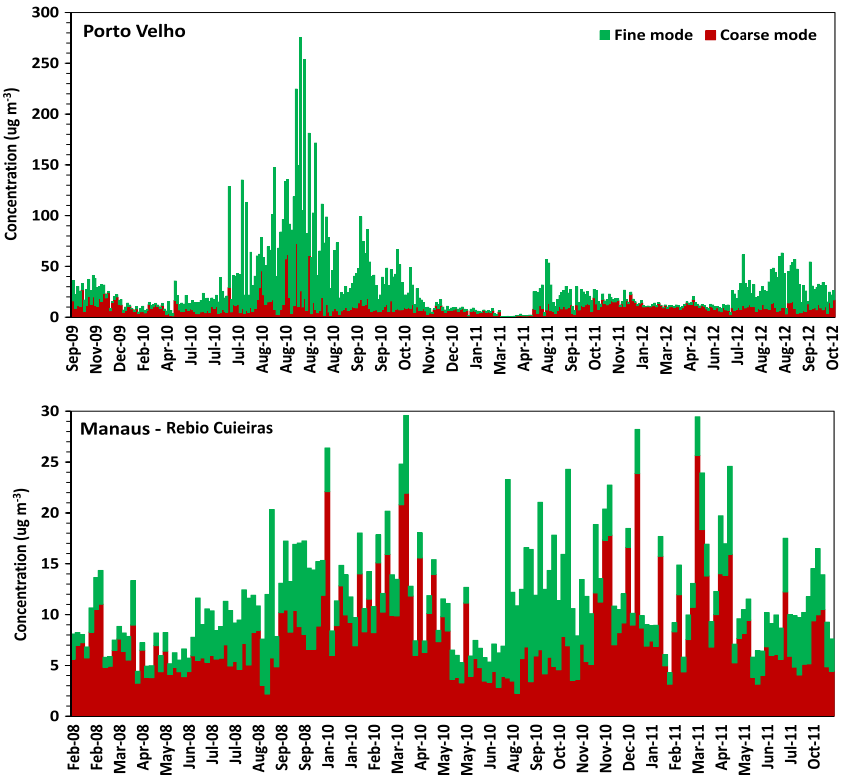

Figure 4. Time series of fine and coarse mode aerosol mass concentrations at Porto Velho perturbed site, from 2009 to 2012, and Manaus pristine site, from 2008 to 2011.

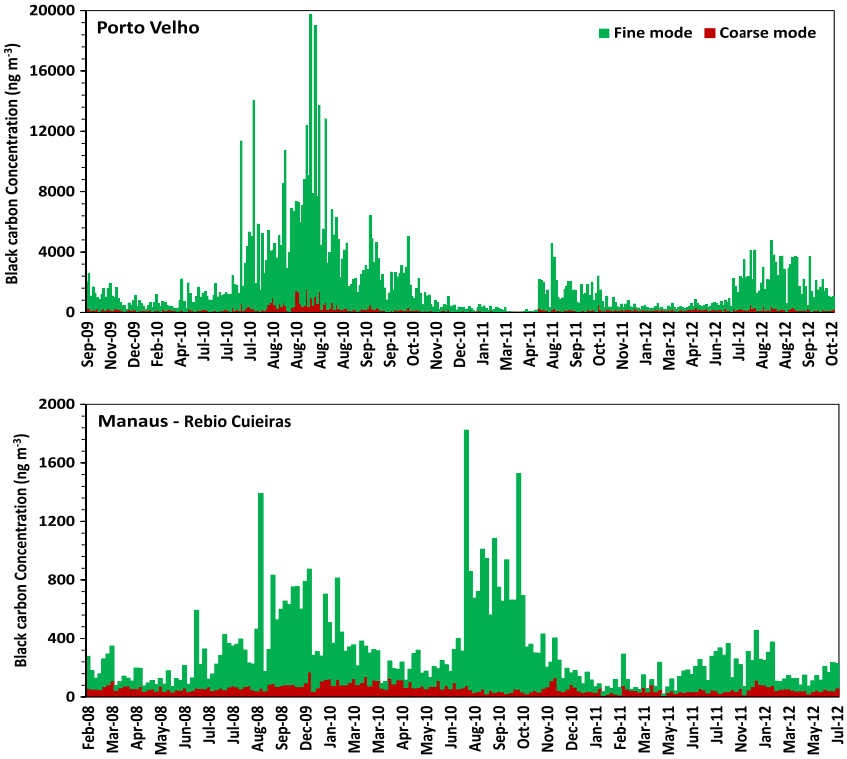

Figure 5. Average aerosol equivalent black carbon concentrations for fine and coarse mode at the Porto Velho, from 2009 to 2012 and Manaus, from 2008 to 2012.

Table 6. Mean concentrations (ng m^{-3}) of particulate matter, equivalent black carbon, and trace elements, in the fine and coarse modes, from filters collected at Manaus—Rebio Cuieiras during the dry and wet seasons are shown

Manaus—Rebio Cuieiras

	Dry Season				Wet Season			
	Fine Mode	*N*	Coarse Mode	*N*	Fine Mode	*N*	Coarse Mode	*N*
PM	7400 ± 4200	39	6000 ± 2500	39	1900 ±1300	63	7600 ± 4500	63
EBC	574 ± 380	39	52 ± 21	39	162 ± 147	63	67 ± 33	63
Na	67 ± 43	22	72 ± 45	22	27 ± 21	32	77 ± 65	34
Mg	15 ± 8	19	25 ± 15	25	24 ± 28	38	31 ± 29	39
Al	31 ± 21	39	41 ± 28	39	76 ± 120	48	69 ± 102	48
Si	36 ± 33	39	56 ± 34	39	138 ± 204	48	140 ± 196	48
P	12 ± 6	39	21 ± 15	39	6.3 ± 3.3	48	47 ± 26	48
S	360 ± 146	39	68 ± 38	39	140 ± 80	48	71 ± 35	48
Cl	4.0 ± 3.4	19	36 ± 39	39	5.7 ± 5.5	32	111 ± 131	48
K	190 ± 115	39	78 ± 49	39	58 ± 42	48	138 ± 70	48
Ca	7.3 ± 3.9	39	19 ± 8	39	13 ± 19	48	29 ± 32	48
Ti	2.1 ± 1.4	33	4.7 ± 2.9	39	5.0 ± 6.0	43	5.3 ± 6.7	48
V	0.4 ± 0.3	15	0.3 ± 0.2	17	0.6 ± 0.7	25	0.3 ± 0.2	24
Cr	0.5 ± 0.6	23	0.4 ± 0.3	27	0.4 ± 0.4	28	0.7 ± 0.6	38
Mn	0.8 ± 1.0	30	0.6 ± 0.4	32	0.7 ± 0.7	45	1.1 ± 0.9	42
Fe	18 ± 10	39	30 ± 14	39	34 ± 52	48	41 ± 54	48
Ni	0.4 ± 0.5	31	0.1 ± 0.2	17	0.5 ± 0.7	43	0.3 ± 0.5	28
Cu	1.3 ± 4.6	30	0.5 ± 0.8	33	0.4 ± 0.6	41	0.5 ± 0.4	45
Zn	1.7 ± 1.1	39	0.9 ± 0.5	39	0.6 ± 0.4	48	1.2 ± 0.6	48
Br	1.5 ± 1.4	36	0.5 ± 0.5	24	0.5 ± 0.5	34	0.5 ± 0.4	33
Rb	0.8 ± 1.3	12	0.6 ± 0.6	8	0.6 ± 0.9	16	0.5 ± 0.5	21
Sr	2.5 ± 2.0	4	2.2 ± 0.0	1	1.0 ± 0.3	2	1.6 ± 2.0	6
Pb	1.6 ± 2.3	22	1.4 ± 1.5	14	1.4 ± 1.4	23	0.7 ± 0.7	19

PM, particulate matter; EBC, equivalent black carbon.
The reported uncertainty is standard deviation of all measurements. The number of samples measured above the detection limit is also given.

validation of the aerosol analysis procedure, hundreds of aerosol samples from Amazonia were analysed. The analysed samples are from clean and pristine areas (Manaus Rebio Cuieiras) and also from areas with heavy biomass burning (Porto Velho, Rondônia). Gravimetric analysis was used to obtain the total mass of the fine and coarse mode particulate matter. At the pristine site, the average fine and coarse mode mass were $4 \pm 3\,\mu g\,m^{-3}$ and $8 \pm 4\,\mu g\,m^{-3}$, respectively, where the uncertainties correspond to the standard deviation of the measurements. In Porto Velho, Rondônia, fine and coarse mode aerosol mass were $21 \pm 32\,\mu g\,m^{-3}$ and $10 \pm 8\,\mu g\,m^{-3}$, respectively, indicating high impact of biomass burning emissions. When distinguishing between the seasons, it was found that the fine mode concentration at the Porto Velho, Rondônia, site was 18 times larger during the dry ($37 \pm 37\,\mu g\,m^{-3}$) than during the wet ($2 \pm 1\,\mu g\,m^{-3}$) season because of the biomass burning aerosols contribution. For the coarse mode, values for the dry ($11 \pm 10\,\mu g\,m^{-3}$) season are slightly larger than for the wet ($7 \pm 4\,\mu g\,m^{-3}$) season. This picture of aerosol concentrations is completely different at the pristine site, which is dominated by natural biogenic aerosol particles. Figure 4 shows the time series of fine and coarse mode mass concentrations for both sites. Concentrations increase only by a factor of 2.5 for the fine mode (from $3 \pm 1\,\mu g\,m^{-3}$ to $8 \pm 4\,\mu g\,m^{-3}$), whereas the coarse mode concentrations are slightly smaller during the dry ($6 \pm 2\,\mu g\,m^{-3}$) than during the wet ($11 \pm 5\,\mu g\,m^{-3}$) season because it is associated with the primary biological aerosol particle emissions.[5] Equivalent black carbon (EBC) analysis was performed using reflectance techniques. Figure 5 shows the time series of fine and coarse mode EBC concentration for both sites. In the fine mode filters during the dry season, it was possible to observe that Porto Velho, Rondônia, showed five times higher concentration of EBC ($3.0 \pm 2.5\,\mu g\,m^{-3}$) compared with Manaus ($0.6 \pm 0.4\,\mu g\,m^{-3}$) confirming the contribution of biomass burning aerosols. For the wet season, the concentrations are similar, $0.3 \pm 0.2\,\mu g\,m^{-3}$ and $0.2 \pm 0.2\,\mu g\,m^{-3}$, respectively, indicating aerosol absorption by natural biogenic aerosol particles.[2]

The elemental composition measured with the EDXRF Epsilon 5, PANalytical B.V. for the fine and coarse mode aerosols at the Manaus site (Table 6) and Porto Velho, Rondônia, site (Table 7) are shown separately for the dry and wet seasons. The mean concentration of trace elements at the Porto Velho site accounted for 8% and 10% of the total particulate matter in the fine mode during the dry and wet seasons, respectively. In the coarse mode, the contribution of the measured elements was 15% (dry) and 5% (wet) of the total mass. At the Manaus site, the elemental contribution to the fine mode total mass was 10% and 20% during the dry and wet seasons, respectively, and 7% and 7% to the coarse mode total mass. This shows that organic aerosols dominate the elemental picture for both sites and both aerosol size fractions.[3]

The aerosol composition in Porto Velho during the dry season is characterized by high concentrations of S and K in the fine mode, associated with EBC, indicating the strong presence of biomass burning aerosols. In the coarse mode, soil dust tracers such as Mg, Al, Si, Ca, Ti, and Fe are systematically found, indicating the presence of soil dust. During the wet season, the natural biogenic emissions are dominant, as shown by the high levels of

Table 7. Mean concentrations (ng m^{-3}) of particulate matter, equivalent black carbon, and trace elements, in the fine and coarse modes, from filters collected at Porto Velho, Rondônia, during the dry and wet seasons

Porto Velho

	Dry Season				Wet Season			
	Fine mode	*N*	Coarse Mode	*N*	Fine Mode	N	Coarse mode	*N*
PM	27900 ± 34100	264	10600 ± 8500	264	1800 ± 1500	90	6900 ± 4200	90
EBC	2347 ± 2753	264	201 ± 210	264	274 ± 270	264	89 ± 58	90
Na	41 ± 50	124	39 ± 45	120	7.1 ± 8.3	102	10 ± 15	106
Mg	26 ± 28	67	52 ± 122	87	5.1 ± 4.5	61	6.5 ± 5.7	81
Al	165 ± 163	209	296 ± 303	201	17 ± 20	150	39 ± 51	142
Si	169 ± 163	209	357 ± 359	207	26 ± 31	150	59 ± 62	145
P	18 ± 12	209	29 ± 30	180	5.0 ± 3.0	150	36 ± 22	150
S	506 ± 446	209	110 ± 123	163	76 ± 69	150	39 ± 27	150
Cl	12 ± 18	87	11 ± 12	128	1.3 ± 2.3	20	12 ± 13	147
K	428 ± 406	209	135 ± 117	209	37 ± 39	150	98 ± 57	150
Ca	15 ± 13	209	39 ± 42	204	3.3 ± 2.8	150	12 ± 9	149
Ti	13 ± 13	209	26 ± 25	205	1.2 ± 1.2	150	3.9 ± 4.6	144
V	1.1 ± 1.7	67	1.4 ± 2.3	88	0.1 ± 0.1	82	0.2 ± 0.1	84
Cr	3.3 ± 4.7	78	2.7 ± 4.2	124	0.4 ± 0.8	54	0.3 ± 0.3	91
Mn	2.2 ± 3.0	119	2.5 ± 3.5	123	0.3 ± 0.2	119	0.5± 0.3	127
Fe	151 ± 147	209	292 ± 277	209	15 ± 15	150	54± 63	150
Ni	1.2 ± 2.3	75	1.1 ± 1.8	30	0.1 ± 0.1	46	0.1 ± 0.1	27
Cu	1.5 ± 2.4	133	1.2 ± 1.9	95	0.7 ± 2.8	129	0.3 ± 0.2	128
Zn	2.9 ± 2.5	170	1.8 ± 1.8	139	0.6 ± 0.9	143	1.1 ± 2.3	147
Br	5.0 ± 7.0	180	2.6 ± 3.7	122	0.5 ± 0.5	115	0.4 ± 0.3	105
Rb	2.3 ± 2.8	133	1.9 ± 3.0	139	0.2 ± 0.2	98	0.4 ± 0.2	99
Sr	8 ± 13	64	9 ± 14	77	1.4 ± 1.2	47	1.6 ± 2.0	52
Pb	5.2 ± 8.6	142	5.0 ± 8.2	147	0.8 ± 0.7	105	0.7 ± 0.8	93

PM, particulate matter; EBC, equivalent black carbon.
The reported uncertainty is standard deviation of all measurements. The number of samples measured above the detection limit is also given.

P, K, Zn, and other elements. In Manaus, high concentrations of S, K, Zn, and P are found during the dry season, indicating a mixture of long-range transported biomass burning and natural biogenic emissions. The concentrations, however, are about half of those measured at Porto Velho because of the lack of local biomass burning aerosols which are mostly transported over large distances. Surprisingly, during the wet season in Manaus, high concentrations of elements associated with soil dust (Al, Si, Ca, Ti, Mn, and Fe) were measured. This has been identified as long-range transport from Sahara dust,[9] transported over the North Atlantic Ocean by the trade winds, what also explains the high concentrations of Cl and Na associated with sea-salt aerosols. The long-range transported dust from Sahara into Amazonia was also observed at the same site using a Raman Lidar instrument[30–32] that showed the dust mixed with biomass burning aerosols from Africa impacting South America tropical regions. It is important to use different techniques for ground-based and remote sensing to identify aerosol components properly.

Conclusion

A calibration procedure for the EDXRF spectrometer of the Laboratory of Atmospheric Physics at the USP was developed, optimizing analysis for trace elements in aerosols. The procedure was optimized for detection of light elements such as Na, Mg, Al, Si, and P, which are important for the scientific issues we deal with. Because of the lack of standards for P, calibration standards were produced in our lab trough the nebulization of salt solutions followed by drying and weighing of Nuclepore filters. A careful calculation of errors in the calibration coefficients of the Epsilon 5, PANalytical B.V. instrument was performed. It was possible to achieve a standard deviation of 2% to 4% for most elements, considering the propagation of the uncertainties in the mass of the standards into the linear fitting of response curves. The DL for the 22 elements measured in our routine analysis were determined by two different methods and compared with values reported in the literature. The proposed methodology to evaluate DLs, on the basis of the standard deviation of repeated samples measurements, has the advantage of including most of the sources of measurement errors giving a more robust estimate. From Na to K, our DLs values are 70% to 50% lower than reported by Spolnik *et al.*[20] for a similar instrument (albeit optimized for heavy elements), whereas from Sr to Pb, our values are larger by a factor of 2. The reproducibility and accuracy of the calibration was verified by measuring several times the NIST 2783 reference material. For most of the elements, our measurements are in good agreement with the certified values, exceptions for Na, S, and Zn. An evaluation of our calibration procedure was undertaken by comparing the elemental concentration in aerosol samples measured in two similar EDXRF instrument at the UA and at CETESB. Agreements better than 10% between these two instruments and our EDXRF were obtained for real aerosol samples. There is an excellent agreement with results from CETESB, which also tuned their Epsilon 5, PANalytical B.V. instrument for detection of light elements. Interlaboratory comparison of EDXRF analysis carried out with real aerosols samples is very valuable for data validation and optimization of different instruments.

The EDXRF measurements of aerosol samples collected at a pristine and a biomass burning impacted area in the Amazon showed very large contributions from elements associated with natural biogenic aerosols during the wet season in both fine and coarse mode size fractions. A strong impact from biomass burning aerosols associated with K, Ca, EBC, and other elements for both sites was observed in the fine mode during the dry season. It was also possible to observe impacts of long-range transported Sahara dust into Amazonia in the wet season for both size fraction, fine, and coarse mode aerosols.[9]

The results from this study showed that the EDXRF Epsilon 5, PANalytical B.V. instrument can be tuned for the measurement of very low concentrations of trace elements typically found in atmospheric aerosols samples collected in Amazonia. Because of the easy sample handling, fast measurement time, and the matrix not being damaged, the EDXRF technique has become our routine elemental composition analysis that is suitable and yields a high accuracy.

Acknowledgements

This research is part of the large-scale biosphere atmosphere experiment in Amazonia that is coordinated by INPA. We would like to thank the INPA LBA central office in Manaus for logistical support for the operation of the Manaus site. This research was funded by the FAPESP projects 2010/52658-1, 2011/50170-4, 2012/14437-9, 2013/05014-0, and CNPq projects 475735/2012-9 and 457843/2013-6. We thank Sandra Hacon (FIOCRUZ), Fernando Morais (IFUSP), Alcides C. Ribeiro (IFUSP), Fábio de Oliveira Jorge (IFUSP), Glauber Cirino (INPA), Lívia Oliveira (INPA), and Junior da Silva (UNIR-Porto Velho) for their technical support and help in keeping the Amazonian sites fully operational.

References

[1] O. Boucher, D. Randall, P. Artaxo, C. Bretherton, G. Feingold, P. Foster, V. Kerminem, Y. Kondo, H. Liao, U. Lohmann, P. Rasch, S. K. Satheesh, S. Sherwood, B. Stevens, X.-Y. Zhang, in *Climate Change 2013: The Physical Science Basis. Working Group I Contribution to the Fifth Assessment Report of the Intergovernmental Panel on Climate Change*, (Eds: S. Fuzzi, J. Penner, V. Ramaswamy, C. Stubenrauch), Cambridge University Press, Stockholm, **2013**, pp. 571–657.
[2] P. Artaxo, L. V. Rizzo, J. F. Brito, H. M. J. Barbosa, A. Arana, E. T. Sena, G. G. Cirino, W. Bastos, S. T. Martin, M. O. Andreae. *Faraday Discuss.* **2013**. doi:10.1039/c3fd00052d.
[3] S. T. Martin, M. O. Andreae, D. Althausen, P. Artaxo, H. Baars, S. Borrmann, Q. Chen, D. K. Farmer, A. Guenther, S. S. Gunthe, J. L. Jimenez, T. Karl, K. Longo, A. Manzi, T. Müller, T. Pauliquevis, M. D. Petters, a. J. Prenni, U. Pöschl, L. V. Rizzo, J. Schneider, J. N. Smith, E. Swietlicki, J. Tota, J. Wang, A. Wiedensohler, S. R. Zorn. *Atmos. Chem. Phys.* **2010**. doi:10.5194/acp-10-11415-2010.
[4] C. Pöhlker, K. T. Wiedemann, B. Sinha, M. Shiraiwa, S. S. Gunthe, M. Smith, H. Su, P. Artaxo, Q. Chen, Y. Cheng, W. Elbert, M. K. Gilles, A. L. D. Kilcoyne, R. C. Moffet, M. Weigand, S. T. Martin, U. Pöschl, M. O. Andreae. *Science* **2012**. doi:10.1126/science.1223264.
[5] U. Pöschl, S. T. Martin, B. Sinha, Q. Chen, S. s. Gunthe, J. A. Huffman, S. Borrmann, D. K. Farmer, R. M. Garland, G. Helas, J. L. Jimenez, S. M. King, A. Manzi, E. Mikhailov, T. Pauliquevis, M. D. Petters, A. J. Prenni, P. Roldin, D. Rose, J. Schneider, H. Su, S. R. Zorn, P. Artaxo, M. O. Andreae. *Science* **2010**. doi:10.1126/science.1191056.
[6] B. Graham, P. Guyon, W. Maenhaut, P. E. Taylor, M. Ebert, S. Matthias-Maser, O. L. Mayol-Bracero, R. H. M. Godoi, P. Artaxo, F. X. Meixner, M. a. L. Moura, C. H. E. D. Rocha, R. Van Grieken, M. M. Glovsky, R. C. Flagan, M. O. Andreae. *J. Geophys. Res. Atmos.* **2003**. doi:10.1029/2003JD004049.
[7] Y. Ben-Ami, I. Koren, Y. Rudich, P. Artaxo, S. T. Martin, M. O. Andreae. *Atmos. Chem. Phys.* **2010**. doi:10.5194/acp-10-7533-2010.
[8] T. Pauliquevis, L. L. Lara, M. L. Antunes, P. Artaxo. *Atmos. Chem. Phys.* **2012**. doi:10.5194/acp-12-4987-2012.
[9] A. Arana, P. Artaxo. *Quim. Nova* **2014**. doi: 10.5935/0100-4042.20140046.
[10] M. O. Andreae. *Science* **2007**. doi:10.1126/science.1136529.
[11] P. Artaxo, J. V. Martins, M. A. Yamasoe, A. S. Procópio, T. Pauliquevis, M. O. Andreae, P. Guyon, L. V. Gatti, A. M. C. Leal. *J. Geophys. Res.* **2002**. doi:10.1029/2001JD000666.

[12] P. Artaxo, C. Q. Orsini. *Nucl. Instruments Methods Phys. Res. Sect. B Beam Interact. with Mater. Atoms* **1987**, *22*, pp. 259–263.
[13] C. Q. Orsini, P. Artaxo, M. H. Tabacniks. *Nucl. Instruments Methods Phys. Res. Sect. B Beam Interact. with Mater. Atoms*. **1984**. doi:10.1016/0168-583X(84)90418-X.
[14] P. K. Hopke, Y. Xie, T. Raunemaa, S. Biegalski, S. Landsberger, W. Maenhaut, P. Artaxo, D. Cohen. *Aerosol Sci. Technol.* **1997**. doi:10.1080/02786829708965507.
[15] I. Nakai, in *X-Ray Spectrometry: Recent Technological Advance*, (Eds: K. Tsuji, J. Injuk, R. Van Grieken), Jonh Wiley and Sons Ltd., England, **2004**, 355–360.
[16] K. Van Meel. *Environ. Chem. Lett.* **2009**. doi:10.1007/s10311-009-0203-4.
[17] I. Szalóki, S. B. Török, C.-U. Ro, J. Injuk, R. E. Van Grieken. *Anal. Chem.* **2000**. doi:10.1021/a1000018h.
[18] L. Kaufman, D. C. Camp. *Adv. X-Ray Anal.* **1975**. doi:10.1007/978-1-4613-9978-0.
[19] P. Standzenieks, E. Selin. *Nucl. Instruments Methods* **1979**. doi:10.1016/0029-554X(79)90308-2.
[20] Z. Spolnik, K. Belikov, K. Van Meel, E. Adriaenssens, F. De Roeck, R. Van Grieken. *Appl. Spectrosc.* **2005**. doi:10.1366/0003702055775142647.
[21] G. Calzolai, M. Chiari, F. Lucarelli, F. Mazzei, S. Nava, P. Prati, G. Valli, R. Vecchi. *Nucl. Instruments Methods Phys. Res. Sect. B Beam Interact. with Mater. Atoms.* **2008**. doi:10.1016/j.nimb.2008.03.056.
[22] A. C. Araújo, A. D. Nobre, B. Kruijt, J. A. Elbers, R. Dallarosa, P. Stefani, C. Von Randow, A. Manzi, A. D. Culf. *J. Geophys. Res. Atmos.* **2002**. doi:10.1029/2001JD000676.
[23] P. Brouwer, *Theory of XRF: Getting Acquainted With the Principles*, PANanalytical B. V, The Netherlands, **2010**, pp. 60.
[24] E. Marguí, R. Padilla, M. Hidalgo, I. Queralt, R. Van Grieken. *X-Ray Spectrom.* **2006**. doi:10.1002/xrs.890.
[25] EPA, *Compendium Method IO-3.3: Determination of Metals in Ambient Particulate Matter Using X-Ray Fluorescence (XRF) Spectroscopy*, EPA, Cincinnati, **1999**, pp. 15–30.
[26] C. Vanhoof, V. Corthouts. *N. De Brucker, Adv. X-Ray Anal.* **2000**, *43*, pp. 449–455.
[27] P. Van Espen, K. Janssens, J. Nobels, *Chemom*, Intell. Lab, Syst, **1986**. doi:10.1016/0169-7439(86)80031-4.
[28] F. Gerab, P. Artaxo, R. Gillett, G. Ayers. *Nucl. Instruments Methods Phys. Res. Sect. B Beam Interact. with Mater. Atoms.* **1998**. doi:10.1016/S0168-583X(97)00887-2.
[29] P. McMurry. *Atmos. Environ.* **2000**. doi:10.1016/S1352-2310(99)00455-0.
[30] A. Ansmann, H. Baars, M. Tesche, D. Müller, D. Althausen, R. Engelmann, T. Pauliquevis, P. Artaxo. *Geophys. Res. Lett.* **2009**. doi:10.1029/2009GL037923.
[31] H. Baars, A. Ansmann, D. Althausen, R. Engelmann, P. Artaxo, T. Pauliquevis, R. Souza. *Geophys. Res. Lett.* **2011**. doi:10.1029/2011GL049200.
[32] H. Baars, A. Ansmann, D. Althausen, R. Engelmann, B. Heese, D. Müller, P. Artaxo, M. Paixao, T. Pauliquevis, R. Souza. *J. Geophys. Res. Atmos.* **2012**. doi:10.1029/2012JD018338.